

# Heterocycles Derived from Generating Monovalent Pnictogens within NCN Pincers and Bidentate NC Chelates: Hypervalency versus Bell-Clappers versus Static Aromatics

Vít Kremláček,<sup>†,‡</sup> Jakub Hývl,<sup>‡,§</sup> Wesley Y. Yoshida,<sup>‡</sup> Aleš Růžička,<sup>†</sup> Arnold L. Rheingold,<sup>§</sup> Jan Turek,<sup>||</sup> Russell P. Hughes,<sup>⊥</sup> Libor Dostál,<sup>\*,†,||</sup> and Matthew F. Cain<sup>\*,‡,||</sup>

<sup>†</sup>Department of General and Inorganic Chemistry, Faculty of Chemical Technology, University of Pardubice, Studentská 573, Pardubice 53210, Czech Republic

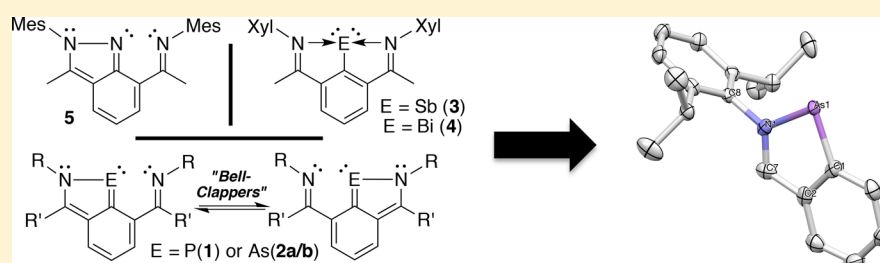
<sup>‡</sup>Department of Chemistry, University of Hawai'i at Mānoa, 2545 McCarthy Mall, Honolulu, Hawaii 96822, United States

<sup>§</sup>Department of Chemistry, University of California, San Diego, 9500 Gilman Drive, La Jolla, California 92093, United States

<sup>||</sup>Enheid Algemene Chemie (ALGC), Vrije Universiteit Brussel (VUB), Pleinlaan 2, B-1050 Brussels, Belgium

<sup>⊥</sup>Department of Chemistry, Dartmouth College, 6128 Burke Laboratory, Hanover, New Hampshire 03755, United States

## S Supporting Information



**ABSTRACT:** Generating monovalent pnictogens within NCN pincers has resulted in the isolation of three distinct types of 1,2-azaheteroles, highly aromatic nitrogen analogues like pyrazole-based **5**, aromatic yet fluxional P- and As-derived bell-clappers **1** and **2**, and hypervalent Sb and Bi derivatives **3** and **4**, which are supported by 3-center, 4-electron N–E–N bonds. Careful analysis of the solid-state structures of **1–5**/[5-Me][OTf] in combination with NICS calculations (at the GIAO/M06/cc-pVTZ(-PP) level) and other computational methods (NBO) suggest that simpler NC chelates may support new phosphorus- and arsenic-containing heterocycles. Indeed, reduction of  $ECl_2$  ( $E = P$  or  $As$ ) derivatives supported by *N*-Dipp (Dipp = 2,6-diisopropylphenyl) substituted NC bidentate ligands produced 1,2-benzoazaphosphole **11** and 1,2-benzoazaarsole **12**. NICS calculations revealed **11** and **12** had aromatic character on par with that of pyrazole-based **5**.

## INTRODUCTION

Five-membered heterocyclic rings,<sup>1</sup> especially those featuring heavier main group elements such as Si,<sup>2</sup> P,<sup>3</sup> Se,<sup>4</sup> and Te<sup>5</sup> have acted as building blocks for the construction of new electronic materials.<sup>6</sup> Phospholes are arguably the most versatile scaffold as the P-substituent can be sterically and electronically varied,<sup>7</sup> the P-lone pair can be functionalized by electrophiles, oxidized, or coordinated to a metal center,<sup>1,6,8</sup> and a plethora of carbon-based substituents can be introduced at the 2,5- and 3,4-positions using the Fagan–Nugent method.<sup>9</sup> Most of the tunability is aimed at careful tweaking of its weakly aromatic character derived from  $\sigma^*-\pi^*$  hyperconjugation between the exocyclic P–R bond and the butadiene unit<sup>10</sup> with the goal of maximizing  $\pi$ -conjugation throughout the organic scaffolding.<sup>1,3,6</sup> Recently, in some of the most promising materials, phosphorus has been replaced by arsenic affording new arsole-based building blocks,<sup>11</sup> permitting direct comparison with their lighter phosphole analogues (Scheme 1).

An alternative approach to maximizing  $\pi$ -conjugation through modification of the  $\sigma^3$ -heteroles is to force the phosphorus or arsenic atoms directly into (p–p) $\pi$  bonding.<sup>12</sup> Unfortunately, the bulky substituents often required to stabilize E=C or E=E double bonds ( $E = P$  or  $As$ ) result in twisting of the structure and reduced  $\pi$ -conjugation,<sup>13</sup> a situation encountered during the synthesis of poly(*p*-phenylenephosphaalkene) (PPP) building blocks,<sup>12</sup> the phosphorus analogue of poly(*p*-phenylenevinylene) (PPV) (Chart 1, top). However, low-coordinate ( $\lambda^3-\sigma^2$ ) phosphorus can be incorporated into ring systems like 1,3-benzoxaphospholes (BOP),<sup>14</sup> 2,6-substituted benzobisoxaphospholes (BBOP),<sup>15</sup> and heteroacene derivatives (NBOP),<sup>16</sup> leading to more extended  $\pi$  networks with advantageous properties such as reversible electrochemical behavior and luminescence/fluorescence with high quantum yields (Chart 1, bottom).

Received: May 4, 2018

## Scheme 1. Phosphole Tunability and Aromaticity

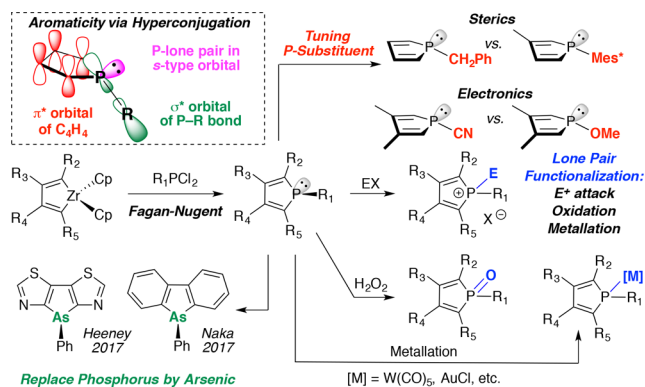
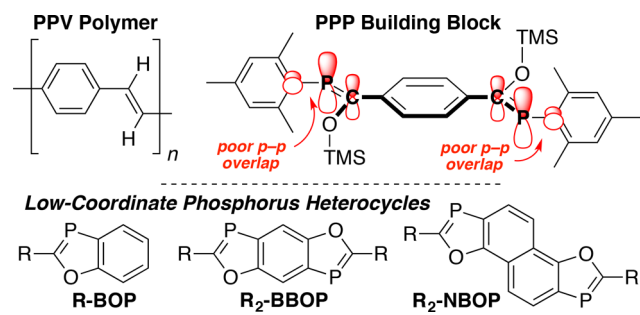


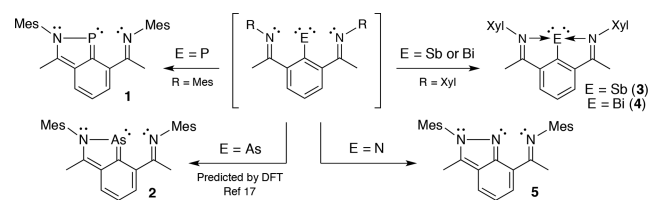
## Chart 1. Comparison of PPV- and PPP-Based Building Blocks and Benzoxazole-Derived Materials



During our efforts to stabilize a phosphinidene within an NCN pincer, we unexpectedly isolated a related, nitrogen-containing 5-membered heterocycle, namely, 1,2-benzoazaphosphole (**1**).<sup>17</sup> Known synthetic routes to 1,2-azaphospholes include vanadium-mediated cycloaddition of phosphalkynes and substituted acetylenes,<sup>18</sup> flash vacuum pyrolysis of 1,2,3,4-triazaphospholes,<sup>19</sup> and Diels–Alder-type reactions between 1,3,2-diazaphosphole-4,5-dicarbonitriles and various acetylenes,<sup>20</sup> all of which are impractical. DFT calculations indicated the As derivative (**2**) should have a similar  $C_s$  symmetric ground-state structure,<sup>17</sup> potentially providing access to a new ring system containing As=C (p–p) $\pi$  bonding.<sup>21</sup> In contrast, Sb(I) and Bi(I) centers formed by reduction<sup>22</sup> within an analogous NCN pincer afforded  $C_{2v}$  symmetric stibinidene **3** and bismuthinidene **4**,<sup>23</sup> hypervalent compounds stabilized by 3-center, 4-electron N–E–N bonds (E = Sb or Bi).<sup>24</sup> The apparent redistribution of electron density observed in **1** and predicted with **2** compared with **3** and **4** suggests that 1,2-azaphospholes and -arsoles may feature weak aromatic character and high  $\pi$  conjugation,<sup>25</sup> ideal monomer properties for the construction of macromolecules.<sup>1,3,6</sup> Generation of the corresponding nitrene was expected to result in trapping by one of the flanking  $sp^2$ -hybridized nitrogen donors<sup>26</sup> affording pyrazole-based **5**, an established aromatic ring system<sup>27</sup> and excellent comparison point for compounds **1**–**4** (Scheme 2).

Here, we report the synthesis of NCN-supported arsenic and nitrogen derivatives **2** and **5**, a comparison of the solid-state structures of **1**–**5** and evaluation of their aromaticity on the basis of NICS calculations, NBO analysis, and by analogy with other related compounds. In addition, we demonstrate that unlike previously reported azaheteroles derived from Sb and Bi 1,2-benzoazaphospholes and 1,2-benzoazaarsoles (**11** and **12**, vide infra) can be supported by simple NC chelates lacking a tethered Lewis base and/or flanking steric protection and are

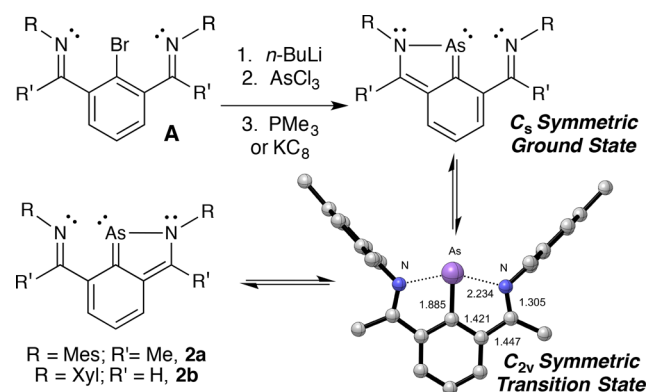
## Scheme 2. Targeted Group 15 Compounds (E = N, P, As, Sb, or Bi)



indeed both isolable and aromatic making them interesting targets as building blocks for future electronic materials.

## RESULTS AND DISCUSSION

**Preparation and Solid-State Structures of 1,2-Azaarsoles 2a/b and Pyrazole-Derived 5.** By analogy to previously reported chemistry with azaphosphole **1**,<sup>17</sup> arsenic derivatives **2a/b** were isolated in 45 and 60% yield, respectively, by sequential addition of *n*-BuLi, AsCl<sub>3</sub>, and either PMe<sub>3</sub> (for **2a**)<sup>28</sup> or KC<sub>8</sub> (for **2b**)<sup>29</sup> to aryl bromides of type **A** (Scheme 3).<sup>30</sup> Both azaarsoles (**2a/b**) exhibited averaged  $C_{2v}$

Scheme 3. Synthesis and Dynamics of 2<sup>a</sup>

<sup>a</sup>The calculated (DFT/B3LYP-D3/LACV3P\*\*) transition state structure of **2a** with selected bond lengths is included.

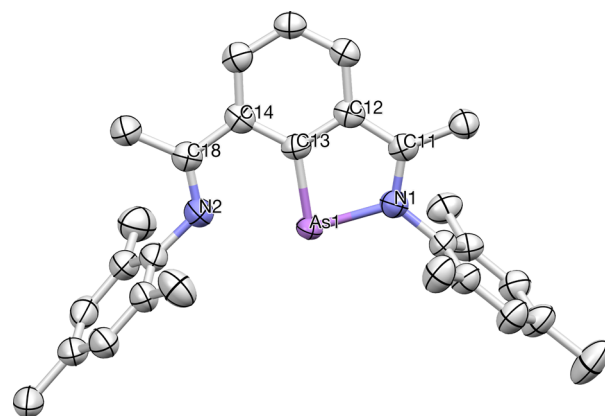


**Figure 1.** X-ray crystal structure of **2a**. Selected bond lengths (Å) and angles (deg): As<sub>1</sub>–N<sub>1</sub> = 1.976(4), As<sub>1</sub>–C<sub>13</sub> = 1.875(4), N<sub>1</sub>–C<sub>11</sub> = 1.321(6), N<sub>2</sub>–C<sub>18</sub> = 1.297(6), C<sub>11</sub>–C<sub>12</sub> = 1.429(6), C<sub>14</sub>–C<sub>18</sub> = 1.469(6), C<sub>13</sub>–C<sub>14</sub> = 1.412(7), C<sub>13</sub>–C<sub>12</sub> = 1.422(6), N<sub>1</sub>–As<sub>1</sub>–C<sub>13</sub> = 82.65(18), As<sub>1</sub>–N<sub>1</sub>–C<sub>11</sub> = 115.6(3). As<sub>1</sub>–N<sub>2</sub> contact: 2.504 Å.

symmetry in solution with a particularly diagnostic downfield-shifted doublet/triplet pattern ( $J = \sim 7.5$  Hz) integrating in

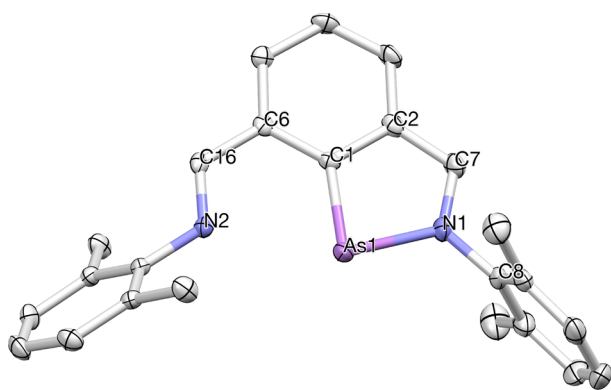
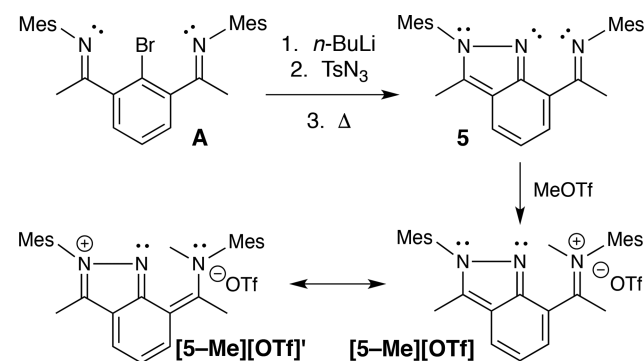


**Figure 2.** X-ray crystal structure of **2b**. Selected bond lengths (Å) and angles (deg): As<sub>1</sub>–N<sub>1</sub> = 1.925(2), As<sub>1</sub>–C<sub>1</sub> = 1.865(2), N<sub>1</sub>–C<sub>7</sub> = 1.334(4), N<sub>2</sub>–C<sub>16</sub> = 1.282(3), C<sub>2</sub>–C<sub>7</sub> = 1.404(3), C<sub>6</sub>–C<sub>16</sub> = 1.453(4), C<sub>1</sub>–C<sub>6</sub> = 1.413(3), C<sub>1</sub>–C<sub>2</sub> = 1.422(4), N<sub>1</sub>–As<sub>1</sub>–C<sub>1</sub> = 82.93(1), As<sub>1</sub>–N<sub>1</sub>–C<sub>7</sub> = 115.34(2). As<sub>1</sub>–N<sub>2</sub> contact: 2.668 Å.

a 2:1 ratio corresponding to the central aromatic protons. These NMR observations are consistent with previous DFT predictions,<sup>17</sup> which suggested azaarsole **2a** would have a C<sub>s</sub> symmetric ground-state structure with a low lying (2.1 kcal/mol) C<sub>2v</sub> symmetric transition state to rapid N<sub>1</sub>–As<sub>1</sub>/As<sub>1</sub>–N<sub>2</sub> bond-switching via a bell-clapper type mechanism.<sup>31</sup> Azaarsole **2b** was also predicted to display a similar low barrier exchange process (**2b** = 1.7 kcal/mol),<sup>32</sup> neither of which can be frozen out by routine VT NMR spectroscopy. Ultimately, their (**2a/b**) unsymmetrical ground state structures were confirmed by X-ray diffraction (Figures 1 and 2, see Table 1 for comparison with 1). Natural Resonance Theory (NRT)<sup>33</sup> indicates that the resonance structures illustrated for compounds **2a/b** and other heavy atom analogues are the most significant contributors to the

#### Scheme 4. Synthesis of **5** and [5-Me][OTf] and Possible Resonance Contributor [5-Me][OTf]'

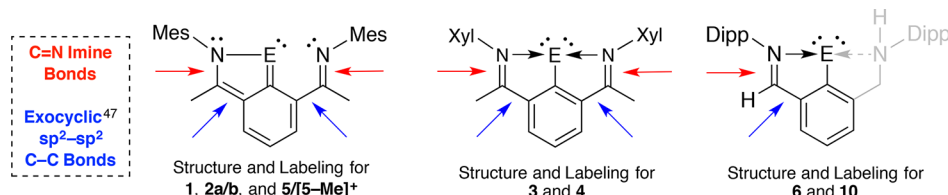


overall resonance hybrid. While the corresponding resonance structure for N-analogue **5** (Scheme 4) is not the principal contributor, it is drawn as such for consistency with its heavy congeners, and all subsequent comparisons use this as the reference structure. Delocalizations from these reference Lewis structures are discussed below (Table 2).

Given the impracticality associated with handling chlorinated amine derivatives,<sup>34</sup> we devised an alternative route to nitrogen counterpart **5**. Lithiation of **A** (R = Mes, R' = Me) with *n*-BuLi, followed by treatment with the electrophilic nitrogen<sup>35</sup> source TsN<sub>3</sub> led to the in situ generation of (NCN)–N<sub>3</sub>, which extruded N<sub>2</sub> upon heating (100 °C) to afford **5** as a colorless oil in 62% yield (Scheme 4).

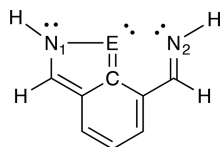
Unlike **1–4**, pyrazole **5** was predicted to and did display an apparent C<sub>s</sub> symmetric structure in solution at room temperature by NMR spectroscopy (Figure 3, left). The <sup>1</sup>H NMR spectrum showed five separate aryl resonances integrating in a

**Table 1.** Selected Bond Lengths and Angles of Compounds **1–5**/[5-Me][OTf], **6**, and **10**<sup>a</sup>



	<b>5</b>	[5-Me] <sup>+</sup>	<b>1</b> <sup>17</sup>	<b>2a</b>	<b>2b</b>	<b>3</b> <sup>23</sup>	<b>4</b> <sup>23</sup>	<b>6</b> <sup>48b</sup>	<b>10</b> <sup>48a</sup>
N–E=C	104.00	102.8(2)	87.81(12)	82.65(18)	82.93(1)	73.60(11) 73.26(11)	71.43(16) 70.83(16)	75.9(2)	76.52(15)
E–N	1.355	1.377(3)	1.757(2)	1.976(4)	1.925(2)	2.352(3) 2.346(3)	2.461(5) 2.464(4)	2.254(5) 2.534(5)	2.230(4)
E–C <sub>Ar</sub>	1.343	1.347(4)	1.744(3)	1.875(4)	1.865(2)	2.052(3)	2.150(5)	2.070(6)	2.222(5)
Exocyclic <sup>47</sup> sp <sup>2</sup> –sp <sup>2</sup> C–C bonds	1.399 1.486	1.409(4) 1.473(4)	1.403(4) 1.474(4)	1.429(6) 1.469(6)	1.404(3) 1.453(4)	1.443(4) 1.451(3)	1.450(7) 1.458(6)	1.451(8)	1.416(5)
C=N Imine Bonds	1.275 1.357	1.297(4) 1.344(4)	1.287(4) 1.350(4)	1.297(6) 1.321(6)	1.282(3) 1.334(4)	1.302(4) 1.300(4)	1.289(7) 1.296(7)	1.338(9)	1.320(7)

<sup>a</sup>The C=N imine bonds and exocyclic sp<sup>2</sup>–sp<sup>2</sup> C–C bonds listed have been labeled for clarity.

Table 2. Selected Atom Hybridizations in a Model NCN Pincer System<sup>a</sup>

E	E <sub>LP</sub>	N <sub>1LP</sub>	N <sub>2LP</sub>	E–N <sub>1</sub> σ	E–C <sub>Ar</sub> σ	N <sub>1</sub> –E σ	C <sub>Ar</sub> –E σ	delocalization N <sub>1LP</sub> → E–C <sub>Ar</sub> π* (kcal/mol)	delocalization N <sub>1LP</sub> → C–Cπ* (kcal/mol)	delocalization N <sub>2LP</sub> → E–N <sub>1</sub> σ* (kcal/mol)
N	sp <sup>1.5</sup>	p	sp <sup>1.7</sup>	sp <sup>2.1</sup>	sp <sup>1.7</sup>	sp <sup>3.5</sup>	sp <sup>2.3</sup>	28.6	37.0	0.0
P	sp <sup>0.4</sup>	p	sp <sup>1.8</sup>	sp <sup>12.7</sup>	sp <sup>3.7</sup>	sp <sup>2.1</sup>	sp <sup>2.4</sup>	10.2	45.4	10.0
As	sp <sup>0.2</sup>	p	sp <sup>2.0</sup>	sp <sup>65</sup>	sp <sup>4.9</sup>	sp <sup>2.0</sup>	sp <sup>2.5</sup>	4.0	66.9	30.6
Sb	sp <sup>0.2</sup>	p	sp <sup>2.0</sup>	sp <sup>100</sup>	sp <sup>5.5</sup>	sp <sup>2.3</sup>	sp <sup>2.6</sup>	2.0	79.2	37.8
Bi	sp <sup>0.1</sup>	p	sp <sup>2.0</sup>	sp <sup>100</sup>	sp <sup>7.9</sup>	sp <sup>2.4</sup>	sp <sup>2.8</sup>	1.5	83.1	36.9

<sup>a</sup>The lone pair on N<sub>1</sub> and the orbitals forming the E–C π-bond are all 100% p.

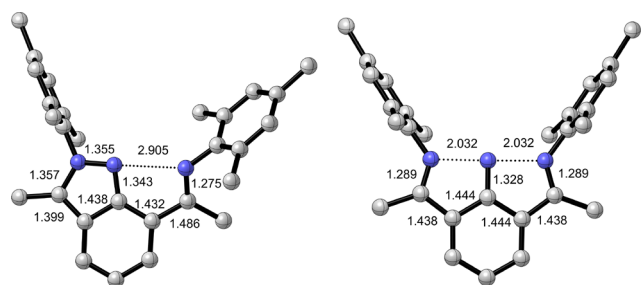


Figure 3. Calculated structure of **5** and predicted TS to bell-clapper type behavior.

1:1:1:2:2 ratio; the central aromatic protons each appeared as doublets of doublets and two separate singlets corresponding to CH protons of N–Mes rings were observed. In addition, six chemically distinct methyl signals were detected, consistent with a structure in which the central nitrogen atom is locked to one side. Despite heating a solution of **5** to 100 °C, the locked structure persisted, indicating the bond-switching process between N<sub>1</sub>–N<sub>2</sub> and N<sub>2</sub>–N<sub>3</sub> must proceed via a high-energy transition state. DFT calculations located this C<sub>2v</sub> transition state 39.4 kcal/mol above the ground state (Figure 3, right),<sup>32</sup> a barrier much higher than associated with analogous P (**1**) and As derivatives (**2a/b**) and inaccessible at 100 °C.

In order to experimentally determine the structure of the pyrazole ring,<sup>36</sup> we quaternized the imine nitrogen (Scheme 4).<sup>37</sup> Addition of MeOTf to a solution of **5** in methylene chloride resulted in crystalline salt [5-Me][OTf] with an unidentified impurity comprising ~10% of the reaction mixture. A combination of <sup>1</sup>H NMR spectroscopy (δ 3.83 and 2.77, *J* = 1.4 Hz) and HSQC and HMBC experiments confirmed the primary site of methylation was at the pendant imine arm and not the central nitrogen atom. Recrystallization of the product mixture from dioxane layered with diethyl ether afforded crystals of [5-Me][OTf] suitable for elemental analysis and X-ray crystallography (Figure 4). In comparison to the calculated structure of **5** (Figure 3, above),<sup>32</sup> the remote methylation altered the structure of the pyrazole-based ring slightly.<sup>36</sup> Quaternization of nitrogen is known to result in the type of C–N bond elongation observed here (1.275 Å in **5** vs 1.297(4) in [5-Me]<sup>+</sup>);<sup>38</sup> however, other minor changes were also observed, including shortening of the C–N pyrazole bond (N<sub>1</sub>–C<sub>10</sub>) accompanied by subsequent lengthening of the adjacent sp<sup>2</sup>–sp<sup>2</sup> C–C bond (C<sub>10</sub>–C<sub>12</sub>) and contracting of the second exocyclic sp<sup>2</sup>–sp<sup>2</sup> C–C bond (C<sub>14</sub>–C<sub>18</sub>, nearest to the quaternized nitrogen).

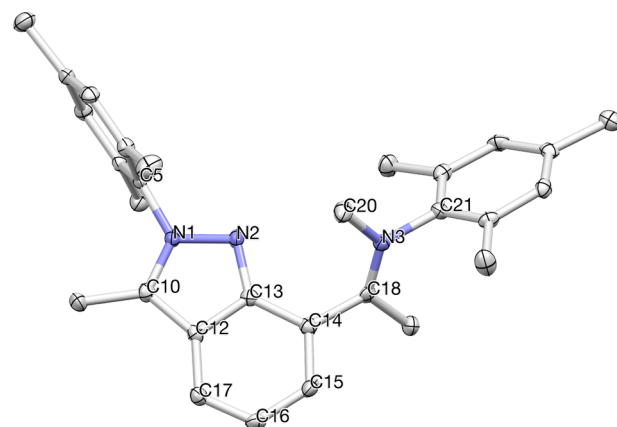


Figure 4. X-ray crystal structure of [5-Me]<sup>+</sup> (anion removed for clarity). Selected bond lengths (Å) and angles (deg): N<sub>2</sub>–C<sub>13</sub> = 1.347(4), N<sub>2</sub>–N<sub>1</sub> = 1.377(3), N<sub>1</sub>–C<sub>10</sub> = 1.344(4), C<sub>10</sub>–C<sub>12</sub> = 1.409(4), C<sub>12</sub>–C<sub>13</sub> = 1.431(4), N<sub>3</sub>–C<sub>18</sub> = 1.297(4), N<sub>3</sub>–C<sub>20</sub> = 1.486(4), C<sub>14</sub>–C<sub>18</sub> = 1.473(4), N<sub>1</sub>–N<sub>2</sub>–C<sub>13</sub> = 102.8(2), N<sub>2</sub>–N<sub>1</sub>–C<sub>10</sub> = 114.8(3).

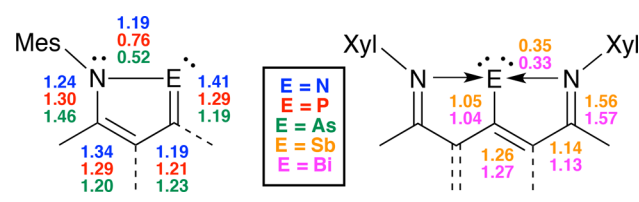
These perturbations are consistent with a contribution from resonance structure [5-Me][OTf]<sup>+</sup> (Scheme 4), reflecting the electronegative nature of the newly methylated nitrogen center. Related indazoles featuring electron-withdrawing groups at the 7-position like 2-allyl-7-nitro-2*H*-indazole have remarkably similar structures.<sup>39</sup>

Selected bond lengths and angles of 1–5/[5-Me][OTf] (and **6** and **10**, *vide infra*) are tallied in Table 1. Consistent with the inability of 3*s*/3*p* and larger atomic orbitals to effectively hybridize,<sup>40</sup> the central atoms in 1–5 are increasingly pyramidalized descending down Group 15 with Bi displaying severely acute N–Bi–C<sub>Ar</sub> angles of 71.13° (avg).<sup>23</sup> Furthermore, in line with well-documented trends for main group compounds, the N–E and E–C bonds lengths increase progressively, from 1.355 Å (N–N) to 2.463 Å (N–Bi average) and from 1.343 Å (N–C) to 2.150(5) Å (Bi–C) as the size of the pnictogen increased,<sup>41</sup> reflecting both increasing p character in the E → N/E → C sigma bonds and the poorer overlap between large p orbitals and the pincer nitrogen and aryl donors (see Table 2 for NBO calculations using the \$CHOOSE keyword along with the reference structure).<sup>42</sup> In fact, hypervalent Sb(I) and Bi(I) analogues **3** and **4** contain virtually no *s*/*p* mixing;<sup>23</sup> the 3-center, 4-electron N–E–N bond<sup>24</sup> involves overlap from two roughly sp<sup>2</sup> hybridized N orbitals and a pure p orbital on the heavy pnictogen.<sup>23</sup> In contrast, the presumed generation of

nitrene,<sup>43</sup> phosphinidene,<sup>44</sup> and arsinidene<sup>45</sup> species following in situ nitrogen extrusion from (NCN)–N<sub>3</sub> or reduction of the (NCN)ECl<sub>2</sub> intermediates (E = P or As) resulted in the isolation of trivalent **5**, **1**, and **2**, respectively. Calculated<sup>32</sup> pyrazole structure **5** and salt [5-Me][OTf] both contained an sp<sup>2</sup> hybridized central nitrogen with a five-membered ring structure deviating only slightly from the parent pyrazole (C<sub>3</sub>H<sub>4</sub>N<sub>2</sub>),<sup>36</sup> featuring significant delocalization of the N<sub>ILP</sub> into the E–C<sub>Ar</sub> π\* bond (Table 2), leading to C–N bond lengths intermediate between single and double bonds.

Results of NBO analyses of model compounds are presented in Table 2. The resonance structure shown was selected as the reference Lewis structure using the \$CHOOSE option in NBO 6.0. Second-order perturbation theory analysis of the Fock matrix in the NBO basis was used to evaluate the stabilization energies associated with delocalizations from this reference structure. The s-character of the lone pair orbital hybridization E<sub>LP</sub> increases dramatically on descending the group. The p-character “lost” from this lone pair is relocated in the σ-bonds from E to its flanking atoms, most significantly in that to N<sub>1</sub>, consistent with Bent’s Rule.<sup>42</sup> As expected, π-delocalization energies for the N<sub>1</sub> p-lone pair electrons into the flanking E–C π\* orbital decrease dramatically on descending the group, yet azaphosphole **1** and azaarsoles **2a/b** still exhibit bond lengths in between E–C<sub>Ar</sub> and E=C<sub>Ar</sub><sup>46</sup> while simultaneously displaying appreciably pyramidalized N–E–C<sub>Ar</sub> bond angles of 87.81(12) and 82.65(18)° (for **2a**; **2b** = N<sub>1</sub>–As<sub>1</sub>–C<sub>1</sub> = 82.93(1), Table 1).<sup>40,42</sup> This is counteracted by an increase in delocalization of the N<sub>1</sub> lone pair into the flanking C–C π\* orbital moving down the pnictogen series. In the structures of **1** and **2a/b**, the exocyclic<sup>47</sup> C=C bond of the five-membered rings remains noticeably short, especially in comparison to the sp<sup>2</sup>–sp<sup>2</sup> C–C bond of the pendant imine donor (Table 1). However, Sb and Bi analogues<sup>23,48</sup> **3** and **4** feature exocyclic C–C bonds of both equal length (within error) and within normal range of sp<sup>2</sup>–sp<sup>2</sup> C–C single bonds,<sup>42</sup> likely due to substantial delocalization of the N<sub>1</sub> lone pair into the C=C π\* orbital (Table 2). Additional, closely related changes were observed at imine functionalities of the NCN pincer. In **5**, **1**, and **2**, the tethered imine unit maintained a short C=N double bond (~1.28 Å), while the imine donor incorporated into the new five-membered rings was significantly elongated (Table 1). Again, no such structural reorganizations were observed with **3** and **4**.<sup>17,23,48</sup> These observations in combination with WBI values<sup>49</sup> highlight that Sb- and Bi-based orbitals ineffectively overlap with their C- and N-based counterparts,<sup>41</sup> resulting in more significant redistribution of electron density from the 6-membered arene ring into the fused 5-membered ring for **5**, **1**, and **2** than in **3** and **4** (Chart 2). This led us to speculate

Chart 2. WBI Values for the Five-Membered Rings in 1–5



that the driving force for the formation of trivalent C<sub>s</sub> symmetric **5**, **2**, and **1** over monovalent C<sub>2v</sub> symmetric **3** and **4** was aromaticity. Furthermore, the increasingly significant delocalization of the N<sub>2</sub> lone pair into the E–N<sub>1</sub> σ\* orbital descending

down group 15 not only is consistent with the transition to the symmetrical ground state structures for Sb and Bi but also provides insight into the origin of the low barrier to N<sub>1</sub>–E/E–N<sub>2</sub> bond exchange via a bell-clapper type process observed even at –60 °C by NMR spectroscopy for **1** and **2a/b**.<sup>17</sup>

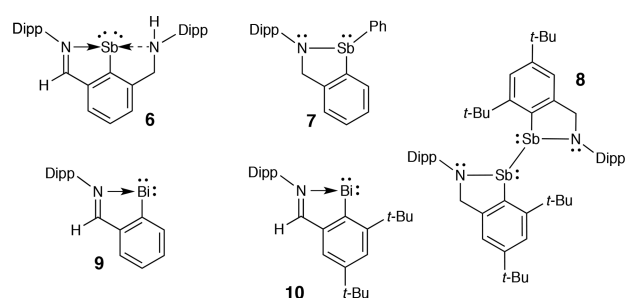
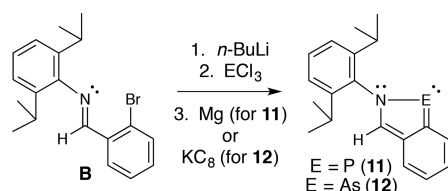
#### Aromaticity and Isolability of Group 15 Heterocycles.

Pyrroles are fully aromatic,<sup>50</sup> while phospholes<sup>1,3,6,10</sup> and arsoles<sup>51</sup> are weakly aromatic, and stiboles and bisboles are increasingly labile.<sup>52</sup> However, their aza-analogues (with the exception of pyrazoles), specifically azaphospholes<sup>17–20</sup> (like **1**) and azaarsoles (like **2a/b**)<sup>21,29</sup> are far less common; therefore, nuclear-independent chemical shift (NICS) calculations (at the GIAO/M06/cc-pVTZ(-PP) level) were performed to gain insight into their aromaticity. Computations were performed at the geometric center (NICS(0)) and at 1 Å above and below (average value NICS(1)) both the five- and six-membered rings, including the out-of-plane component (NICS(1)<sub>zz</sub>), which is often considered the best gauge of aromaticity.<sup>53</sup> Of the series of group 15 azaheteroles (**1**–**5**), the pyrazole unit (C<sub>3</sub>NN ring) in **5** was the most aromatic, displaying even more negative (aromatic) NICS values than benzene (Table 3). Azaphosphole **1** (C<sub>3</sub>NP) was more aromatic than were azaarsoles **2a/b** (C<sub>3</sub>NAs), but both were less aromatic than the pyrazole. In contrast, the fused nitrogen-containing five-membered rings of hypervalent Sb (**3**, C<sub>3</sub>NSb) and Bi (**4**, C<sub>3</sub>NBi) derivatives exhibited low aromaticity, consistent with the lack of hybridization at the central atom, weak 3-center, 4-electron N–E–N bonds (E = Sb or Bi), and negligible redistribution of electron density between the heavy atom and the pincer scaffold. In fact, only recently have “non-hypervalent” azastibole derivatives **6**–**8**<sup>48b</sup> and azabisboles **9**<sup>54</sup> and **10**<sup>48a</sup> been reported (Chart 3).

Antimony-derived **6**, featuring a five-membered C<sub>3</sub>NSb ring with significant aromatic character is the singly hydrogenated analogue of NCN pincer ligated **3** (with Dipp substituents on nitrogen instead of Xyl), possessing a noticeably longer Sb–C bond and unequally contributing nitrogen donors (see Table 1 for **6** and **10**).<sup>48b</sup> Interestingly, despite substantial flanking steric bulk, preparation of an Sb(I) species without the second nitrogen donor resulted in dimerization to trivalent **8**.<sup>48b</sup> Single-arm **7** containing a related Sb(III) center, an sp<sup>3</sup> benzylic carbon, and amido and phenyl donors is a nonaromatic five-membered ring system and only unsupported azastibole known to date.<sup>48b,55</sup> On the contrary, singly ligated Bi(I) species **9** can be generated, but in the absence of trapping agents (RE–ER, E = S, Se, and Te) to afford Bi(III) species, decomposes into unidentifiable product mixtures.<sup>54</sup> However, if considerable steric bulk is placed at the ortho and para positions of the fused benzene ring, then **10** is isolable.<sup>48a</sup> Intriguingly, some structural reorganization like that present in **5**, **1**, and **2** did occur. The exocyclic sp<sup>2</sup>–sp<sup>2</sup> C–C bond was short, and the C=N imine bond was long with NICS calculations indicating appreciably more aromatic character was present in **10** versus **4** but was still less in comparison to those in **1** and **2a/b**.<sup>48a</sup> Furthermore, the Bi–C bond remained composed of almost entirely p character, showing insignificant multiple bonding (WBI = 1.05)<sup>48a</sup> and the presence of a high-energy p-type lone pair, which may account for its reactivity in the absence of neighboring steric bulk. Given **1** and **2** represented lighter analogues of **9**, but with a secondary E–N contact like that in **6** (in **1**, P–N contact = 2.676 Å; in **2a**, As–N contact = 2.504 Å; in **6**, long Sb–N bond = 2.534(5) Å), we speculated if aromatic character alone in the absence of any additional steric (large *t*-Bu groups

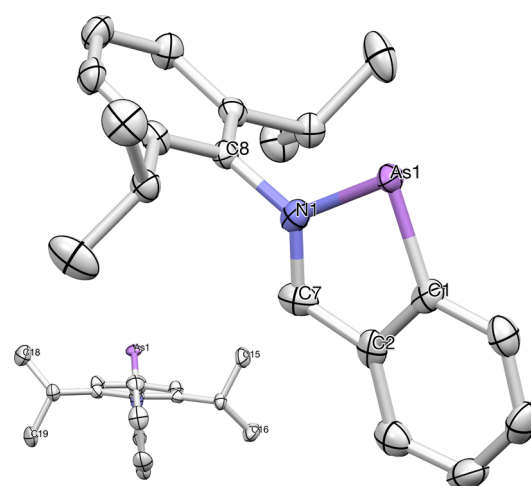
**Table 3.** GIAO/M06/cc-pVTZ(-PP) Computed NICS (ppm) for the Five- And Six-Membered Rings in Compounds **1**, **2a/b**, **3–5**, **[5-Me]<sup>+</sup>**, and **10–12**

compound		C <sub>3</sub> NE ring			C <sub>6</sub> ring		
		NICS(0)	NICS(1)	NICS(1) <sub>zz</sub>	NICS(0)	NICS(1)	NICS(1) <sub>zz</sub>
<b>1</b>	E = P	-10.3	-9.5	-26.8	-5.9	-8.1	-21.1
<b>2a</b>	E = As	-8.0	-7.8	-20.7	-6.0	-8.2	-21.6
<b>2b</b>	E = As	-9.7	-8.9	-25.2	-5.9	-8.0	-21.6
<b>3</b> <sup>48a</sup>	E = Sb	-3.2, -3.2	-4.2, -4.2	-8.8, -8.8	-6.2	-8.6	-22.8
<b>4</b> <sup>48a</sup>	E = Bi	-2.8, -2.8	-3.9, -3.9	-7.3, -7.3	-6.4	-8.8	-23.0
<b>5</b>	E = N	-13.2	-11.7	-34.4	-6.8	-8.3	-21.6
<b>[5-Me]<sup>+</sup></b>	E = N	-12.7	-11.4	-32.7	-6.7	-8.4	-21.6
<b>6</b> <sup>48b</sup>	E = Sb	-8.7	-7.9	-21.5	-5.9	-8.2	-22.0
<b>10</b> <sup>48a</sup>	E = Bi	-8.1	-7.1	-17.5	-6.6	-8.6	-21.2
<b>11</b>	E = P	-12.9	-10.9	-31.9	-6.8	-8.8	-24.0
<b>12</b>	E = As	-11.9	-10.2	-29.4	-6.7	-8.7	-23.6
benzene	reference				-8.4	-10.4	-29.8

**Chart 3.** Azastibole and Azabisole Derivatives **6–10****Scheme 5.** Synthesis of **11** and **12**

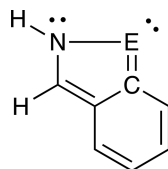
on the central ring, i.e., **10**) or electronic stabilization (second nitrogen donor, i.e., **6**) would render azaphospholes and azarsoles isolable.

**Synthesis of Unsupported 1,2-Benzoazaphospholes and 1,2-Benzoazaarsoles.** To this end, azaphosphole **11** and azaarsole **12** featuring unsubstituted, fused benzene rings and single imine donors to the pnictogen center were targeted. Azaphosphole **11** was previously isolated and structurally characterized by Tokitoh as the unexpected byproduct in the attempted synthesis of phosphorus analogues of the  $\beta$ -diketiminato ligands.<sup>56</sup> Here, its rational synthesis along with As counterpart **12** was achieved by treatment of **B**<sup>57</sup> with *n*-BuLi, followed by quenching with ECl<sub>3</sub> (E = P or As) and in situ reduction with Mg or KC<sub>8</sub>, affording both compounds as analytically pure yellow solids in 24 and 51% yield, respectively (Scheme 5). In solution, **11** and **12** exhibited apparent C<sub>s</sub> symmetry with six downfield-shifted aryl protons and a seventh imine signal integrating in a 1:1:1:1:2:1:1 ratio. In addition, two separate signals for the *i*-Pr methyl groups were observed by both <sup>1</sup>H and <sup>13</sup>C{<sup>1</sup>H} NMR spectroscopy, likely due to restricted rotation about the (sp<sup>2</sup>)C<sub>Ar</sub>-CH(CH<sub>3</sub>)<sub>2</sub> bonds leaving one set of methyl groups pointed above the five-membered As-containing ring and other pair directed below. X-ray quality crystals confirmed the structure of **12** with the inset of Figure 5 highlighting the orientation of the *i*-Pr methyl groups.

**Figure 5.** X-ray crystal structure of **12**. Selected bond lengths (Å) and angles (deg): As<sub>1</sub>-C<sub>1</sub> = 1.865(5), As<sub>1</sub>-N<sub>1</sub> = 1.883(6), N<sub>1</sub>-C<sub>8</sub> = 1.452(8), N<sub>1</sub>-C<sub>7</sub> = 1.308(7), C<sub>7</sub>-C<sub>2</sub> = 1.419(9), C<sub>2</sub>-C<sub>1</sub> = 1.417(9), N<sub>1</sub>-As<sub>1</sub>-C<sub>1</sub> = 83.8(2), As<sub>1</sub>-N<sub>1</sub>-C<sub>7</sub> = 115.5(4).**Table 4.** Selected Bond Lengths (Å) and Bond Angles (deg) of **11** and **12**

	<b>11</b> <sup>56</sup>	<b>12</b>
N-E=C	88.1(3)	83.8(2)
E-N	1.702(10)	1.883(6)
E-C <sub>Ar</sub>	1.744(4)	1.868(5)
exocyclic <sup>47</sup> sp <sup>2</sup> -sp <sup>2</sup> C-C bond	1.416(7)	1.419(9)
shared sp <sup>2</sup> -sp <sup>2</sup> C-C bond	1.426(6)	1.417(9)
C=N imine bond	1.334(10)	1.308(7)

Interestingly, the E-C<sub>Ar</sub> bond lengths in azaphospholes **1** and **11** and azaarsoles **2** and **12** were the same within error (Tables 4 and 1), indicative of similar redistribution of electron density within the fused ring system and corroborated by remarkably similar E-C<sub>Ar</sub> hybridizations and delocalizations of the N lone pair into the E-C π\* orbital as determined by NBO calculations using the reference structure illustrated in Table 5 (compare with Table 2). However, the lack of the destabilizing N<sub>2LP</sub> → E-N<sub>1</sub> σ\* interaction from the flanking imine donor in **11** and **12** resulted in significantly shorter (>0.05 Å) N-E bonds with increased s character (E → N) versus **1** and **2**. A related but less drastic N-E bond contraction (0.02 Å) was observed on comparing pincer ligated

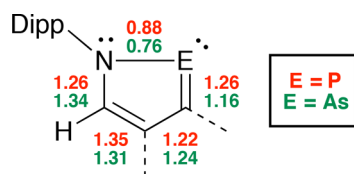
Table 5. Selected Atom Hybridizations in a Model NC Bidentate System<sup>a</sup>

E	E <sub>LP</sub>	E–N $\sigma$	E–C $\sigma$	N–E $\sigma$	C–E $\sigma$	delocalization N <sub>LP</sub> $\rightarrow$ E–C $\pi^*$ (kcal/mol)	delocalization N <sub>LP</sub> $\rightarrow$ C–C $\pi^*$ (kcal/mol)
N	sp <sup>1.5</sup>	sp <sup>3.5</sup>	sp <sup>1.7</sup>	sp <sup>2.1</sup>	sp <sup>2.3</sup>	27.2	38.6
P	sp <sup>0.4</sup>	sp <sup>7.7</sup>	sp <sup>4.0</sup>	sp <sup>2.1</sup>	sp <sup>2.5</sup>	11.7	40.8
As	sp <sup>0.3</sup>	sp <sup>13.6</sup>	sp <sup>6.0</sup>	sp <sup>2.2</sup>	sp <sup>2.6</sup>	6.9	48.5
Sb	sp <sup>0.2</sup>	sp <sup>17.7</sup>	sp <sup>7.9</sup>	sp <sup>2.2</sup>	sp <sup>2.8</sup>	4.0	54.6
Bi	sp <sup>0.1</sup>	sp <sup>27.2</sup>	sp <sup>11.1</sup>	sp <sup>2.3</sup>	sp <sup>2.9</sup>	3.1	59.1

<sup>a</sup>The lone pair on N<sub>1</sub> and the orbitals forming the E–C  $\pi$ -bond are all 100% p.

Bi-based **4** with its structurally characterized single-arm derivative **10**. However, unlike the Bi case where the disparity in N–Bi bond lengths could be attributed to 2-center, 2-electron bonding in **10** versus notoriously weak and hypervalent 3-center, 4-electron bonding in **4**,<sup>24</sup> the structural differences between **1** and **11** and **2** and **12** are linked to aromaticity. NICS calculations revealed **11** was more aromatic than **12**, but both C<sub>3</sub>NE five-membered rings were almost as aromatic as the pyrazole in **5**, dwarfing the aromaticity of **1** and **2a/b** (Table 3)! Of the remaining bonds in the azaphosphole ring in **11**, the exocyclic<sup>47</sup> sp<sup>2</sup>–sp<sup>2</sup> C–C bond shortened (1.416(7) Å) and the C=N bond lengthened (1.334(10) Å), but not as dramatically as those in **1** (1.403(4) and 1.350(4) Å). However, azaarsole **12** featured a C–C bond (1.419(9) Å) intermediate between pincer derivatives **2a** (1.429(6) Å) and **2b** (1.404(3) Å) with only a marginally elongated C=N bond (1.308(7) Å versus 1.321(6) Å in **2a** and 1.334(4) Å in **2b**). Finally, the shared sp<sup>2</sup>–sp<sup>2</sup> C–C bond joining the five- and six-membered rings in **11** and **12** is the same length within error as the exocyclic<sup>47</sup> sp<sup>2</sup>–sp<sup>2</sup> C–C bond.

WBI values corroborate the widespread delocalization of electron density and intermediacy of single and double bonds in the five-membered rings of **11** and **12** (Chart 4, compared

Chart 4. WBI Values for the Five-membered Rings in **11** and **12**

with Chart 2). This type of bond length equalization in combination with the planarity of the fused ring system,<sup>53</sup> the isolability and low reactivity compared with **9/10**,<sup>48a</sup> and the strikingly negative NICS values make a strong case for azaphosphole **11** and azaarsole **12** to be considered bona fide aromatic heterocycles. Upcoming studies will ascertain if **11** and **12** exhibit reactivity consistent with a 6 $\pi$  electron (or 10 $\pi$  including the fused benzene unit) heterocycle or a 1,3-diene.

## CONCLUSION

Using methodology closely related to the preparation of **1**, azaarsoles **2a/b** and pyrazole-based **5** were synthesized and fully characterized, adding to the growing number of compounds derived from generating pnictogens in the +1 oxidation

state within an NCN pincer.<sup>17,23,48</sup> These heterocycles range from static and highly aromatic **5** (and its salt [5-Me][OTf]) to aromatic, but fluxional bell-clappers **1** and **2a/b** to hypervalent and weakly aromatic **3** and **4**, containing 3-center, 4-electron N–E–N bonds (E = Sb or Bi). Previous efforts showed that if Sb(I) or Bi(I) species were supported by bidentate NC chelates that dimerization (**8**) or unidentified decomposition pathways occurred (**9**) unless significant steric protection was employed (**10**). Here, we demonstrated that the analogous P(I) and As(I) intermediates undergo a redistribution of electron density similar to those of **1** and **2a/b**, affording trivalent benzoazaphospholes **11** and **12**. These heterocycles display aromatic character on par with pyrazole-derived **5**, resulting in an apparent “line in the sand” between As and Sb in which simple five-membered 6 $\pi$  electron heterocycles can or cannot be isolated. Future investigations will explore if more sterically and electronically diverse benzoazaphospholes and -arsoles can be synthesized and if they can be employed as novel building blocks for new electronic materials.

## EXPERIMENTAL SECTION

**General Experimental Details.** Unless otherwise specified, all reactions and manipulations were performed under a nitrogen atmosphere in a MBraun glovebox or using standard Schlenk techniques. All glassware was oven-dried overnight (at minimum) at 140 °C prior to use. Anhydrous solvents were purchased directly from chemical suppliers (Aldrich or Acros), pumped directly into the glovebox and stored over oven-activated 4 or 5 Å molecular sieves (Aldrich) or were dried using Pure Solv–Innovative Technology equipment and stored over molecular sieves in reservoirs equipped with Teflon Young valves. Aryl bromides of types **A** and **B** were prepared by previously published methods.<sup>30,57</sup> AsCl<sub>3</sub>, *n*-BuLi, MeOTf, and PCl<sub>3</sub> were purchased from commercial suppliers. PMe<sub>3</sub> was obtained from Strem Chemicals and stored over 4 Å molecular sieves in a Schlenk bomb equipped with a screw-top Teflon cap. NMR spectra were obtained on either Varian spectrometers operating at 300 or 500 MHz or Bruker 400 and 500 MHz spectrometers; all spectra are displayed in the Supporting Information. NMR chemical shifts are reported as ppm relative to tetramethylsilane and are referenced to the residual proton or <sup>13</sup>C signal of the solvent (<sup>1</sup>H CDCl<sub>3</sub>, 7.27 ppm; <sup>1</sup>H C<sub>6</sub>D<sub>6</sub>, 7.16 ppm; <sup>13</sup>C CDCl<sub>3</sub>, 77.16 ppm; <sup>13</sup>C C<sub>6</sub>D<sub>6</sub>, 128.06 ppm). Mass spectroscopic data was obtained on an Agilent 6545 Accurate-Mass Q-TOF LC/MS (NSF CHE-1532310). Analytical data were obtained from the CENTC Elemental Analysis Facility at the University of Rochester, funded by NSF CHE-065–456 or on a LECO–CHNS-932 analyzer. All X-ray quality crystals were analyzed at the Small Molecular X-ray Crystallography Facility located at the University of California, San Diego.

**Synthesis of 2a.** Aryl bromide **A**<sup>30</sup> (R = Mes, R' = Me, 800 mg, 1.68 mmol) was dissolved in THF (100 mL) and cooled to –78 °C. A solution of 1.6 M *n*-BuLi in hexanes (1.2 mL, 1.92 mmol, 1.1 equiv)

was added dropwise to the precooled solution and stirred at  $-78\text{ }^{\circ}\text{C}$  for 10 min. Subsequently, a solution of  $\text{AsCl}_3$  (660 mg, 3.64 mmol, 2.2 equiv) in THF (10 mL) was added to the reaction mixture, stirred at  $-78\text{ }^{\circ}\text{C}$  for 10 min, and then stirred at r.t. for 1 h. The volatiles were then removed from the reaction mixture under reduced pressure. The obtained residue was washed with *n*-pentane ( $2 \times 75\text{ mL}$ ), suspended in THF (50 mL), and treated with  $\text{PMe}_3$  (450 mg, 5.92 mmol, 3.5 equiv), leading to an intense purple reaction mixture. The reaction mixture was stirred at r.t. for 2 h, and the volatiles were removed under reduced pressure. The obtained residue was extracted with toluene ( $4 \times 25\text{ mL}$ ), the extracts were combined and filtered through a Celite plug, and the filtrate was concentrated under reduced pressure. The crude purple product was dissolved in  $\text{CH}_3\text{CN}$  (50 mL), filtered through a Celite plug, and the filtrate was concentrated to  $\sim 20\text{ mL}$  and kept at  $-30\text{ }^{\circ}\text{C}$  overnight. Purple crystals were then collected by filtration (359 mg, 0.763 mmol, 45%). Anal. Calcd for  $\text{C}_{28}\text{H}_{31}\text{AsN}_2$ : C, 71.48; H, 6.64; N, 5.95. Found: C, 71.64; H, 6.81; N, 5.65.  $^1\text{H NMR}$  (500 MHz,  $\text{CDCl}_3$ ):  $\delta$  8.11 (d,  $J = 7.6\text{ Hz}$ , 2H), 7.36 (t,  $J = 7.6\text{ Hz}$ , 1H), 6.95 (s, 4H), 2.39 (s, 6H), 2.33 (s, 6H), 2.02 (s, 12H).  $^{13}\text{C}\{^1\text{H}\}$  NMR (126 MHz,  $\text{CDCl}_3$ ):  $\delta$  163.35, 157.62, 142.36, 134.50, 133.10, 130.10, 128.68 (CH), 128.56 (CH), 119.57 (CH), 21.02 ( $\text{CH}_3$ ), 18.55 ( $\text{CH}_3$ ), 15.41 ( $\text{CH}_3$ ).

**Synthesis of 2b.** First, 1.478 g (3.5 mmol) of aryl bromide A ( $\text{R} = \text{Xyl}$ ,  $\text{R}' = \text{H}$ ) was dissolved in 200 mL of diethyl ether, cooled to  $-78\text{ }^{\circ}\text{C}$ , and 2.2 mL of *n*-BuLi (3.5 mmol, 1.6 M solution in hexanes) was added. The resulting mixture was stirred for an additional 30 min at  $-78\text{ }^{\circ}\text{C}$  and then added to a precooled ( $-78\text{ }^{\circ}\text{C}$ ) solution of  $\text{AsCl}_3$  (0.3 mL, 3.5 mmol) in 100 mL of diethyl ether. The reaction mixture was stirred for 24 h at r.t., resulting in the formation of a yellow precipitate. Subsequently, the mixture was concentrated (to ca. 50 mL), the solution was filtered off, and the remaining yellow solid was dried in vacuo. This solid was dissolved in 150 mL of THF and freshly prepared  $\text{KC}_8$  from 0.738 g (61.5 mmol, 10% excess) of graphite, and 0.333 g (8.5 mmol, 20% excess) of potassium was added. The reaction mixture was stirred overnight at r.t. Thereafter, the mixture was evaporated in vacuo and extracted with 200 mL of hexane. The red extracted solution was concentrated to ca. 20 mL and crystallized at  $-30\text{ }^{\circ}\text{C}$  giving a red microcrystalline solid characterized as  $\{\text{C}_6\text{H}_3\text{-2,6-}[\text{CH}=\text{NC}_6\text{H}_3\text{-2',6'-(CH}_3)_2]\}_2\text{As}$ . X-ray quality single-crystals were obtained by recrystallization from a saturated hexane solution. Yield: 0.870 g (60%, 2.1 mmol), mp  $145\text{ }^{\circ}\text{C}$ . Anal. Calcd for  $\text{C}_{24}\text{H}_{23}\text{AsN}_2$  ( $M_w$  414.37): C 69.6, H 5.5, N 6.8. Found: C 69.3, H 5.6, N 6.6%.  $^1\text{H NMR}$  (500 MHz,  $\text{C}_6\text{D}_6$ ,  $25\text{ }^{\circ}\text{C}$ ):  $\delta$  2.08 (s, 12H,  $\text{CH}_3$ ), 6.98 (m, 6H,  $\text{C}_6\text{H}_3(\text{CH}_3)_2\text{-H}_{3,4,5}$ ), 7.08 (t,  $^3J(^1\text{H},^1\text{H}) = 7.5\text{ Hz}$ , 1H,  $\text{C}_6\text{H}_3\text{-H}_4$ ), 7.57 (d,  $^3J(^1\text{H},^1\text{H}) = 7.5\text{ Hz}$ , 2H,  $\text{C}_6\text{H}_3\text{-H}_{3,5}$ ), 7.99 (s, 2H,  $\text{CH}=\text{N}$ ) ppm.  $^{13}\text{C}\{^1\text{H}\}$  NMR (126 MHz,  $\text{C}_6\text{D}_6$ ,  $25\text{ }^{\circ}\text{C}$ ):  $\delta$  18.61 (s,  $\text{C}_6\text{H}_3(\text{CH}_3)_2$ ), 121.2 (s,  $\text{C}_6\text{H}_3\text{-C}_4$ ), 126.3 (s,  $\text{C}_6\text{H}_3\text{-C}_{3,5}$ ), 128.7 (s,  $\text{C}_6\text{H}_3(\text{CH}_3)_2\text{-C}_{3,5}$ ), 130.7 (s,  $\text{C}_6\text{H}_3(\text{CH}_3)_2\text{-C}_4$ ), 131.2 (s,  $\text{C}_6\text{H}_3(\text{CH}_3)_2\text{-C}_{2,6}$ ), 134.3 (s,  $\text{C}_6\text{H}_3(\text{CH}_3)_2\text{-C}_1$ ), 148.3 (s,  $\text{C}_6\text{H}_3\text{-C}_{2,6}$ ), 152.7 (s,  $\text{CH}=\text{N}$ ), 165.7 (s,  $\text{C}_6\text{H}_3\text{-C}_1$ ) ppm.

**Synthesis of 5.** Aryl bromide A ( $\text{R} = \text{Mes}$ ,  $\text{R}' = \text{Me}$ , 800 mg, 1.68 mmol) was dissolved in THF (100 mL) and cooled to  $-78\text{ }^{\circ}\text{C}$ . A 1.6 M *n*-BuLi solution in hexanes (1.1 mL, 1.77 mmol, 1.05 equiv) was added dropwise to the solution and stirred at  $-78\text{ }^{\circ}\text{C}$  for 10 min. Subsequently, a solution of tosylazide ( $\text{TsN}_3$ , 400 mg, 2.03 mmol, 1.2 equiv) in 10 mL of THF was added dropwise to the reaction mixture, stirred at  $-78\text{ }^{\circ}\text{C}$  for 10 min, and then at r.t. for 1 h. The reaction was quenched by addition of water (2 mL). The volatiles were removed under reduced pressure, and the resulting intermediate azide ( $\text{NCN}$ ) $\text{-N}_3$  was purified by column chromatography (silica gel, mobile phase with polarity gradient from ethyl acetate/*n*-hexane 1:10 to 1:8,  $R_f = 0.24$  at 1:8 ratio). The isolated azide ( $\text{NCN}$ ) $\text{-N}_3$  (548 mg, 1.25 mmol) was used in the following step.  $^1\text{H NMR}$  (300 MHz,  $\text{CDCl}_3$ ):  $\delta$  7.68 (d,  $J = 7.6\text{ Hz}$ , 2H), 7.41 (m, 1H), 6.91 (s, 4H), 2.30 (s, 6H), 2.14 (s, 12H), 2.12 (s, 6H). The azide ( $\text{NCN}$ ) $\text{-N}_3$  (548 mg, 1.25 mmol) was dissolved in  $\text{CHCl}_3$  (10 mL) and stirred at  $100\text{ }^{\circ}\text{C}$  for 2 h in Schlenk flask sealed with a Teflon screw cap. The organic volatiles were removed under reduced pressure, and the resulting crude product was purified by column chromatography (silica gel, mobile phase: ethyl acetate/*n*-hexane 1:10;  $R_f = 0.23$ ).

The title product (428 mg, 1.05 mmol) was obtained in 62% overall yield. Anal. Calcd for  $\text{C}_{28}\text{H}_{31}\text{N}_3$ : C, 82.11; H, 7.63; N, 10.26. Found: C, 81.73; H, 7.61; N, 9.67.  $^1\text{H NMR}$  (500 MHz,  $\text{CDCl}_3$ ):  $\delta$  8.05 (dd,  $J = 7.0, 1.0\text{ Hz}$ , 1H), 7.78 (dd,  $J = 8.3, 1.0\text{ Hz}$ , 1H), 7.20 (dd,  $J = 8.3, 7.0\text{ Hz}$ , 1H), 7.04 (s, 2H), 6.89 (s, 2H), 2.43 (s, 3H), 2.41 (s, 3H), 2.39 (s, 3H), 2.30 (s, 3H), 2.10 (s, 6H), 1.91 (s, 6H).  $^{13}\text{C}\{^1\text{H}\}$  NMR (126 MHz,  $\text{CDCl}_3$ ):  $\delta$  168.50, 147.08, 146.52, 139.48, 135.75, 135.58, 132.82, 131.68, 130.39, 129.13 (CH), 128.94, 128.55 (CH), 126.05 (CH), 122.34 (CH), 121.99, 120.60 (CH), 21.36 ( $\text{CH}_3$ ), 21.30 ( $\text{CH}_3$ ), 20.90 ( $\text{CH}_3$ ), 18.09 ( $\text{CH}_3$ ), 17.34 ( $\text{CH}_3$ ), 9.95 ( $\text{CH}_3$ ).

**Synthesis of [5-Me][OTf].** A solution of methyl triflate (156 mg, 0.95 mmol, 0.95 equiv) in DCM (4 mL) was added dropwise to a stirring solution of 5 (410 mg, 1.00 mmol) in DCM (6 mL). The reaction mixture was stirred at r.t. for 2 h, and the volatiles were removed under reduced pressure. The obtained residue was triturated in  $\text{Et}_2\text{O}$  (6 mL) and stirred overnight affording a solid, which was collected by filtration, washed with  $\text{Et}_2\text{O}$  ( $3 \times 10\text{ mL}$ ), and dried under vacuum. The crude product was recrystallized twice from a solution of 1,4-dioxane layered with  $\text{Et}_2\text{O}$ . The title product (243 mg, 0.42 mmol) was obtained as yellow (X-ray quality) crystals in 42% yield. Major compound: Anal. Calcd for  $\text{C}_{30}\text{H}_{34}\text{F}_3\text{N}_3\text{O}_3\text{S}$ : C, 62.81; H, 5.97; N, 7.32. Found: C, 62.58; H, 5.89; N, 7.03.  $^1\text{H NMR}$  (500 MHz,  $\text{CDCl}_3$ ):  $\delta$  8.21 (dd,  $J = 7.1, 0.7\text{ Hz}$ , 1H), 8.09 (dd,  $J = 8.4, 0.7\text{ Hz}$ , 1H), 7.42 (dd,  $J = 8.4, 7.1\text{ Hz}$ , 1H), 7.07–7.03 (m, 4H), 3.83 (d,  $J = 1.4\text{ Hz}$ , 3H), 2.77 (d,  $J = 1.4\text{ Hz}$ , 3H), 2.45 (s, 3H), 2.39 (s, 3H), 2.35 (s, 6H), 2.33 (s, 3H), 1.85 (s, 6H).  $^{13}\text{C NMR}$  (126 MHz,  $\text{CDCl}_3$ ):  $\delta$  188.47 (q,  $\text{C}=\text{N}^+$ ), 143.32, 141.10, 140.21, 138.60, 135.84, 134.92, 134.85, 132.10 (CH), 131.07, 130.87 (CH), 129.35 (CH), 128.60 (CH), 121.79, 120.94 (CH), 119.69, 48.08 ( $\text{CH}_3$ ), 26.58 ( $\text{CH}_3$ ), 21.29 ( $\text{CH}_3$ ), 21.12 ( $\text{CH}_3$ ), 17.25 (two overlapping  $\text{CH}_3$ ), 10.08 ( $\text{CH}_3$ ).  $^{19}\text{F NMR}$  (471 MHz,  $\text{CDCl}_3$ ):  $\delta$   $-78.88$  ( $\text{OSO}_2\text{CF}_3$ ). Minor compound:  $^1\text{H NMR}$  (500 MHz,  $\text{CDCl}_3$ ):  $\delta$  8.74 (d,  $J = 7.5\text{ Hz}$ , 1H), 8.38 (d,  $J = 8.3\text{ Hz}$ , 1H), 7.62–7.54 (m, 1H), 7.07–7.05 (m, 4H), 3.69 (s, 6H), 2.88 (s, 3H), 2.54 (s, 3H), 2.38 (s, 3H), 2.16 (s, 6H), 1.88 (s, 6H).

**Synthesis of 11.**<sup>56</sup> First, 4.111 g (11.9 mmol) of aryl bromide **B**<sup>57</sup> was dissolved in 250 mL of diethyl ether, cooled to  $-78\text{ }^{\circ}\text{C}$ , and 7.47 mL of *n*-BuLi (11.9 mmol, 1.6 M solution in hexanes) was added. The solution was stirred at  $-78\text{ }^{\circ}\text{C}$  for an additional 1.5 h, resulting in the formation of a yellow precipitate. This mixture was then added to 1.04 mL of  $\text{PCl}_3$  (11.9 mmol) in 100 mL of diethyl ether precooled to  $-78\text{ }^{\circ}\text{C}$ . The reaction mixture was stirred at room temperature for 1.5 h, then evaporated in vacuo yielding a green precipitate, which was subsequently dissolved in 200 mL of THF and treated with 0.319 g (13.1 mmol, 10% excess) of magnesium, activated with a small amount of 1,2-dibromoethane. The reaction mixture was stirred at r.t. overnight and evaporated in vacuo. The residue was extracted with hexane (200 mL), and the extract was concentrated and crystallized at  $-30\text{ }^{\circ}\text{C}$  affording a yellowish precipitate of  $\{\text{C}_6\text{H}_4\text{-2-}[\text{CH}=\text{NC}_6\text{H}_3\text{-2',6'-(i-Pr)}_2]\}_2\text{P}$ . Yield: 0.844 g (24%, 2.9 mmol), mp  $113\text{ }^{\circ}\text{C}$ . Anal. Calcd for  $\text{C}_{19}\text{H}_{22}\text{NP}$  ( $M_w$  295.358): C 77.3, H 7.5, N 10.5; Found: C 77.5, H 7.8, N 10.8%.  $^{31}\text{P}\{^1\text{H}\}$  NMR (161.9 MHz,  $\text{C}_6\text{D}_6$ ,  $25\text{ }^{\circ}\text{C}$ ):  $\delta$  182.8 ppm.  $^1\text{H NMR}$  (500 MHz,  $\text{C}_6\text{D}_6$ ,  $25\text{ }^{\circ}\text{C}$ ):  $\delta$  0.98 (d,  $^3J(^1\text{H},^1\text{H}) = 6.9\text{ Hz}$ , 6H,  $\text{CH}_3$ ), 1.12 (d,  $^3J(^1\text{H},^1\text{H}) = 6.9\text{ Hz}$ , 6H,  $\text{CH}_3$ ), 2.38 (septet,  $^3J(^1\text{H},^1\text{H}) = 6.9\text{ Hz}$ , 2H,  $(\text{CH}_3)_2\text{CH}$ ), 6.93 (m, 1H,  $\text{C}_6\text{H}_4\text{-H}_5$ ), 7.00 (m, 1H,  $\text{C}_6\text{H}_4\text{-H}_4$ ), 7.07 (d,  $^3J(^1\text{H},^1\text{H}) = 7.8\text{ Hz}$ , 2H,  $\text{C}_6\text{H}_3\text{-H}_4$ ), 7.22 (t,  $^3J(^1\text{H},^1\text{H}) = 7.8\text{ Hz}$ , 1H,  $\text{C}_6\text{H}_3\text{-H}_{3,5}$ ), 7.58 (d,  $^nJ(^{31}\text{P},^1\text{H}) = 3.9\text{ Hz}$ , 1H,  $\text{CH}=\text{N}$ ), 7.70 (d,  $^3J(^1\text{H},^1\text{H}) = 8.6\text{ Hz}$ , 1H,  $\text{C}_6\text{H}_4\text{-H}_3$ ), 7.99 (dd,  $^3J(^1\text{H},^1\text{H}) = 8.5\text{ Hz}$ ,  $^3J(^{31}\text{P},^1\text{H}) = 3.3\text{ Hz}$ , 1H,  $\text{C}_6\text{H}_4\text{-H}_6$ ) ppm.  $^{13}\text{C}\{^1\text{H}\}$  NMR (125.8 MHz,  $\text{C}_6\text{D}_6$ ,  $25\text{ }^{\circ}\text{C}$ ):  $\delta$  25.2 (s,  $\text{CH}_3$ ), 25.8 (s,  $\text{CH}_3$ ), 28.7 (s,  $(\text{CH}_3)_2\text{CH}$ ), 123.1 (d,  $^3J(^{31}\text{P},^{13}\text{C}) = 18.5\text{ Hz}$ ,  $\text{C}_6\text{H}_4\text{-C}_5$ ), 123.6 (d,  $^4J(^{31}\text{P},^{13}\text{C}) = 3.7\text{ Hz}$ ,  $\text{C}_6\text{H}_4\text{-C}_4$ ), 124.0 (s,  $\text{C}_6\text{H}_3\text{-C}_{3,5}$ ), 124.7 (d,  $^3J(^{31}\text{P},^{13}\text{C}) = 1.8\text{ Hz}$ ,  $\text{C}_6\text{H}_4\text{-C}_3$ ), 125.5 (d,  $^2J(^{31}\text{P},^{13}\text{C}) = 19.8\text{ Hz}$ ,  $\text{C}_6\text{H}_4\text{-C}_6$ ), 129.8 (s,  $\text{C}_6\text{H}_3\text{-C}_4$ ), 131.8 (d,  $^2J(^{31}\text{P},^{13}\text{C}) = 7.3\text{ Hz}$ ,  $\text{C}_6\text{H}_4\text{-C}_2$ ), 135.9 (d,  $^nJ(^{31}\text{P},^{13}\text{C}) = 7.4\text{ Hz}$ ,  $\text{CH}=\text{N}$ ), 139.1 (d,  $^2J(^{31}\text{P},^{13}\text{C}) = 10.1\text{ Hz}$ ,  $\text{C}_6\text{H}_3\text{-C}_1$ ), 146.4 (d,  $^3J(^{31}\text{P},^{13}\text{C}) = 1.8\text{ Hz}$ ,  $\text{C}_6\text{H}_3\text{-C}_{2,6}$ ), 159.1 (d,  $^1J(^{31}\text{P},^{13}\text{C}) = 40.9\text{ Hz}$ ,  $\text{C}_6\text{H}_4\text{-C}_1$ ) ppm.

**Synthesis of 12.** First, 2.367 g (5.8 mmol) of  $\{\text{C}_6\text{H}_4\text{-2-}[\text{CH}=\text{NC}_6\text{H}_3\text{-2',6'-(i-Pr)}_2]\}_2\text{AsCl}_2$ <sup>58</sup> was dissolved in 150 mL of THF and

2 equiv of  $\text{KC}_8$  freshly prepared from 1.210 g (100.8 mmol, 10% excess) of graphite, and 0.542 g (13.9 mmol, 20% excess) of potassium were added. The resulting mixture was stirred at r.t. overnight, evaporated in vacuo, and extracted with 200 mL of hexane. The yellow extracted solution was concentrated to ca. 30 mL and crystallized at  $-30^\circ\text{C}$ . Compound  $\{\text{C}_6\text{H}_4\text{-}2\text{-}[\text{CH}=\text{NC}_6\text{H}_3\text{-}2',6'\text{-}(\text{i-Pr})_2]\text{As}\}$  was obtained in the form of yellow microcrystalline solid. X-ray quality single-crystals were obtained by recrystallization from diethyl ether. Yield: 1.002 g (51%, 2.9 mmol), mp  $126^\circ\text{C}$ . Anal. Calcd for  $\text{C}_{19}\text{H}_{22}\text{AsN}$  ( $M_w$  339.306): C 67.3, H 6.5, N 4.1; Found: C 67.6, H 6.3, N 4.2%.  $^1\text{H}$  NMR (500 MHz,  $\text{C}_6\text{D}_6$ ,  $25^\circ\text{C}$ ):  $\delta$  0.98 (d,  $^3J(\text{H}^1, \text{H}^1) = 6.9$  Hz, 6H,  $\text{CH}_3$ ), 1.13 (d,  $^3J(\text{H}^1, \text{H}^1) = 6.8$  Hz, 6H,  $\text{CH}_3$ ), 2.51 (septet,  $^3J(\text{H}^1, \text{H}^1) = 6.9$  Hz, 2H,  $(\text{CH}_3)_2\text{CH}$ ), 6.90 (t,  $^3J(\text{H}^1, \text{H}^1) = 7.3$  Hz, 1H,  $\text{C}_6\text{H}_4\text{-H}_5$ ), 7.00 (t,  $^3J(\text{H}^1, \text{H}^1) = 7.7$  Hz, 1H,  $\text{C}_6\text{H}_4\text{-H}_4$ ), 7.08 (d,  $^3J(\text{H}^1, \text{H}^1) = 7.8$  Hz, 2H,  $\text{C}_6\text{H}_3\text{-H}_4$ ), 7.22 (t,  $^3J(\text{H}^1, \text{H}^1) = 7.8$  Hz, 1H,  $\text{C}_6\text{H}_3\text{-H}_{3,5}$ ), 7.80 (d,  $^3J(\text{H}^1, \text{H}^1) = 8.6$  Hz, 1H,  $\text{C}_6\text{H}_4\text{-H}_3$ ), 7.89 (s, 1H,  $\text{CH}=\text{N}$ ), 8.02 (d,  $^3J(\text{H}^1, \text{H}^1) = 8.4$  Hz, 1H,  $\text{C}_6\text{H}_4\text{-H}_6$ ) ppm.  $^{13}\text{C}\{\text{H}\}$  NMR (125.8 MHz,  $\text{C}_6\text{D}_6$ ,  $25^\circ\text{C}$ ):  $\delta$  25.3 (s,  $\text{CH}_3$ ), 25.8 (s,  $\text{CH}_3$ ), 28.5 (s,  $(\text{CH}_3)_2\text{CH}$ ), 123.0 (overlap of two signals,  $\text{C}_6\text{H}_4\text{-C}_{4,5}$ ), 124.0 (s,  $\text{C}_6\text{H}_3\text{-C}_{3,5}$ ), 127.3 (s,  $\text{C}_6\text{H}_4\text{-C}_3$ ), 127.4 (s,  $\text{C}_6\text{H}_4\text{-C}_6$ ), 129.3 (s,  $\text{C}_6\text{H}_3\text{-C}_4$ ), 132.7 (s,  $\text{C}_6\text{H}_4\text{-C}_2$ ), 141.3 (s,  $\text{C}_6\text{H}_3\text{-C}_1$ ), 141.8 (s,  $\text{CH}=\text{N}$ ), 145.5 (s,  $\text{C}_6\text{H}_3\text{-C}_{2,6}$ ), 172.2 (s,  $\text{C}_6\text{H}_4\text{-C}_1$ ) ppm.

**DFT Calculations.** DFT and associated NBO calculations were run using the Jaguar suite of programs;<sup>59</sup> full details are provided in the Supporting Information.

**NICS Calculations.** The GIAO/M06/cc-pVTZ(-PP) (Table 3) and GIAO/B3LYP/6-311++G\*\* (Table S1) methods were used for the NICS (nucleus-independent chemical shifts) calculations. Geometries optimized at the M06/cc-pVDZ(-PP) level were taken for the former, while the B3LYP-D3/6-311++G\*\* optimized geometries were considered for the latter. NICS values were calculated at the geometrical center of the five- and six-membered rings [NICS(0)] and at 1 Å above and below the ring center [average value NICS(1)]. The NICS descriptors of benzene at the respective level are also included as a reference. The out-of-plane component for this tensor [NICS(1)<sub>zz</sub>] was also evaluated. NICS are negative (diamagnetic) for aromatic compounds and positive (paramagnetic) for antiaromatic systems.

**X-ray Crystallography.** See the Supporting Information for details.

## ■ ASSOCIATED CONTENT

### Supporting Information

The Supporting Information is available free of charge on the ACS Publications website at DOI: 10.1021/acs.organomet.8b00290.

Complete experimental details supplemented with NMR spectra and specifics on DFT computational methodology; optimized Cartesian coordinates (PDF)

### Accession Codes

CCDC 1842544–1842547 contain the supplementary crystallographic data for this paper. These data can be obtained free of charge via [www.ccdc.cam.ac.uk/data\\_request/cif](http://www.ccdc.cam.ac.uk/data_request/cif), or by emailing [data\\_request@ccdc.cam.ac.uk](mailto:data_request@ccdc.cam.ac.uk), or by contacting The Cambridge Crystallographic Data Centre, 12 Union Road, Cambridge CB2 1EZ, UK; fax: +44 1223 336033.

## ■ AUTHOR INFORMATION

### Corresponding Authors

\*E-mail: [libor.dostal@upce.cz](mailto:libor.dostal@upce.cz).

\*E-mail: [mfcain@hawaii.edu](mailto:mfcain@hawaii.edu).

### ORCID

Libor Dostál: 0000-0002-5982-1239

Matthew F. Cain: 0000-0002-0673-5839

### Author Contributions

#V.K. and J.H. contributed equally to this work.

## Notes

The authors declare no competing financial interest.

## ■ ACKNOWLEDGMENTS

M.F.C. thanks the University of Hawai'i at Mānoa (UHM) for generous start-up funds and laboratory space. Mass spectroscopic data was obtained at UHM on an Agilent 6545 Accurate-Mass QTOF-LCMS (NSF CHE-1532310). L.D. thanks the Czech Science Foundation for continuous support project no. 18-10222S. J.T. acknowledges the financial support of the Research Foundation—Flanders (FWO); Project No. 12Y7718N) and the computational resources and services provided by the Shared ICT Services Centre funded by the Vrije Universiteit Brussel, the Flemish Supercomputer Center (VSC) and FWO. R.P.H. thanks Prof. Eric Glendening (Indiana State University) for help with some NBO CHOOSE settings. Elemental analyses were conducted by William Brennessel (University of Rochester).

## ■ REFERENCES

- Baumgartner, T. *Acc. Chem. Res.* **2014**, *47*, 1613–1622.
- Zhao, Z.; He, B.; Tang, B. Z. *Chem. Sci.* **2015**, *6*, 5347–5365.
- Shameem, M. A.; Orthaber, A. *Chem. - Eur. J.* **2016**, *22*, 10718–10735.
- Heeney, M.; Zhang, W.; Crouch, D. J.; Chabinyk, M. L.; Gordeyev, S.; Hamilton, R.; Higgins, S. J.; McCulloch, I.; Skabara, P. J.; Sparrowe, D.; Tierney, S. *Chem. Commun.* **2007**, 5061–5063.
- Carrera, E. I.; Seferos, D. S. *Macromolecules* **2015**, *48*, 297–308.
- Baumgartner, T.; Réau, R. *Chem. Rev.* **2006**, *106*, 4681–4727.
- (a) Coggon, P.; Engel, J. F.; McPhail, A. T.; Quin, L. D. *J. Am. Chem. Soc.* **1970**, *92*, 5779–5780. (b) Keglevich, G.; Böcskei, Z.; Keserü, G. M.; Ujszászy, K.; Quin, L. D. *J. Am. Chem. Soc.* **1997**, *119*, 5095–5099. (c) Mattmann, E.; Mathey, F.; Sevin, A.; Frison, G. *J. Org. Chem.* **2002**, *67*, 1208–1213.
- Mathey, F. *Chem. Rev.* **1988**, *88*, 429–453.
- (a) Fagan, P. J.; Nugent, W. A. *J. Am. Chem. Soc.* **1988**, *110*, 2310–2312. (b) Fagan, P. J.; Nugent, W. A.; Calabrese, J. C. *J. Am. Chem. Soc.* **1994**, *116*, 1880–1889. (c) Yan, X.; Xi, C. *Acc. Chem. Res.* **2015**, *48*, 935–946. (d) Broene, R. D.; Buchwald, S. L. *Science* **1993**, *261*, 1696–1701.
- Wu, J.; Wu, S.; Geng, Y.; Yang, G.; Muhammad, S.; Jin, J.; Liao, Y.; Su, Z. *Theor. Chem. Acc.* **2010**, *127*, 419–427.
- (a) Tanaka, S.; Imoto, H.; Yumura, T.; Naka, K. *Organometallics* **2017**, *36*, 1684–1687. (b) Imoto, H.; Sasaki, H.; Tanaka, S.; Yumura, T.; Naka, K. *Organometallics* **2017**, *36*, 2605–2611. (c) Green, J. P.; Cryer, S. J.; Marafie, J.; White, A. J. P.; Heeney, M. *Organometallics* **2017**, *36*, 2632–2636.
- Wright, V. A.; Patrick, B. O.; Schneider, C.; Gates, D. P. *J. Am. Chem. Soc.* **2006**, *128*, 8836–8844.
- (a) Shah, S.; Concolino, T.; Rheingold, A. L.; Protasiewicz, J. D. *Inorg. Chem.* **2000**, *39*, 3860–3867. (b) Wu, S.; Deligonal, N.; Protasiewicz, J. D. *Dalton Trans.* **2013**, *42*, 14866–14874.
- Washington, M. P.; Gudimetla, V. B.; Laughlin, F. L.; Deligonal, N.; He, S.; Payton, J. L.; Simpson, M. C.; Protasiewicz, J. D. *J. Am. Chem. Soc.* **2010**, *132*, 4566–4567.
- Washington, M. P.; Payton, J. L.; Simpson, M. C.; Protasiewicz, J. D. *Organometallics* **2011**, *30*, 1975–1983.
- Laughlin, F. L.; Deligonal, N.; Rheingold, A. L.; Golen, J. A.; Laughlin, B. J.; Smith, R. C.; Protasiewicz, J. D. *Organometallics* **2013**, *32*, 7116–7121.
- Hylv, J.; Yoshida, W. Y.; Rheingold, A. L.; Hughes, R. P.; Cain, M. F. *Chem. - Eur. J.* **2016**, *22*, 17562–17565.
- Peters, C.; Tabellion, F.; Schröder, M.; Bergsträßer, U.; Preuss, F.; Regitz, M. *Synthesis* **2000**, *2000*, 417–428.
- Rösch, W.; Facklam, T.; Regitz, M. *Tetrahedron* **1987**, *43*, 3247–3256.

- (20) Karaghiosoff, K.; Klehr, H.; Schmidpeter, A. *Chem. Ber.* **1986**, *119*, 410–419.
- (21) For information on related azarsoles: Pfeifer, G.; Papke, M.; Frost, D.; Sklorz, J. A. W.; Habicht, M.; Müller, C. *Angew. Chem., Int. Ed.* **2016**, *55*, 11760–11764. and the references therein.
- (22) Alternative methods of reducing RECl<sub>3</sub> derivatives: (a) Norton, E. L.; Szekeley, K. L. S.; Dube, J. W.; Bomben, P. G.; Macdonald, C. L. B. *Inorg. Chem.* **2008**, *47*, 1196–1203. (b) Dube, J. W.; Farrar, G. J.; Norton, E. L.; Szekeley, K. L. S.; Cooper, B. F. T.; Macdonald, C. L. B. *Organometallics* **2009**, *28*, 4377–4384. (c) Martin, C. D.; Ragogna, P. *J. Dalton Trans.* **2011**, *40*, 11976–11980. (d) Dube, J. W.; Ragogna, P. *J. Chem. - Eur. J.* **2013**, *19*, 11768–11775.
- (23) Simon, P.; de Proft, F.; Jambor, R.; Ruzicka, A.; Dostál, L. *Angew. Chem., Int. Ed.* **2010**, *49*, 5468–5471.
- (24) Akiba, K.; Moriyama, Y.; Mizozoe, M.; Inohara, H.; Nishii, T.; Yamamoto, Y.; Minoura, M.; Hashizume, D.; Iwasaki, F.; Takagi, N.; Ishimura, K.; Nagase, S. *J. Am. Chem. Soc.* **2005**, *127*, 5893–5901.
- (25) Hoeben, F. J. M.; Jonkheijm, P.; Meijer, E. W.; Schenning, A. P. H. *J. Chem. Rev.* **2005**, *105*, 1491–1546.
- (26) (a) Ning, R. Y.; Madan, P. B.; Sternbach, L. H. *J. Org. Chem.* **1973**, *38*, 3995–3998. (b) Potts, K. T.; Marshall, J. L. *J. Org. Chem.* **1976**, *41*, 129–133.
- (27) Krygowski, T. M.; Anulewicz, R.; Cyranski, M. K.; Puchala, A.; Rasala, D. *Tetrahedron* **1998**, *54*, 12295–12300.
- (28) Hyvl, J.; Yoshida, W. Y.; Moore, C. E.; Rheingold, A. L.; Cain, M. F. *Polyhedron* **2018**, *143*, 99–104.
- (29) Compound **2c** (R = *t*-Bu; R' = H) was previously proposed to have a C<sub>2v</sub> symmetric ground state structure: Vranova, I.; Kremlacek, V.; Erben, M.; Turek, J.; Jambor, R.; Ruzicka, A.; Alonso, M.; Dostál, L. *Dalton Trans.* **2017**, *46*, 3556–3568. The combination of NMR spectroscopy, DFT calculations, and X-ray crystallography have now unequivocally demonstrated its ground state structure is C<sub>s</sub> symmetric.
- (30) Stol, M.; Snelders, D. J. M.; Godbole, M. D.; Havenith, R. W. A.; Haddleton, D.; Clarkson, G.; Lutz, M.; Spek, A. L.; van Klink, G. P. M.; van Koten, G. *Organometallics* **2007**, *26*, 3985–3994.
- (31) (a) Martin, J. C.; Basalay, R. J. *J. Am. Chem. Soc.* **1973**, *95*, 2572–2578. (b) Forbus, T. R.; Martin, J. C. *J. Am. Chem. Soc.* **1979**, *101*, 5057–5059.
- (32) See the [Experimental Section](#) and the [Supporting Information](#) for computational details.
- (33) (a) Glendening, E. D.; Weinhold, F. *J. Comput. Chem.* **1998**, *19*, 593–609. (b) Glendening, E. D.; Weinhold, F. *J. Comput. Chem.* **1998**, *19*, 610–627. (c) Glendening, E. D.; Badenhop, J. K.; Weinhold, F. *J. Comput. Chem.* **1998**, *19*, 628–646.
- (34) Trogolo, D.; Arey, J. S. *Phys. Chem. Chem. Phys.* **2015**, *17*, 3584–3598.
- (35) (a) Erdik, E. *Tetrahedron* **2004**, *60*, 8747–8782. (b) For a related recent example, see Bukhryakov, K. V.; Schrock, R. R.; Hoveyda, A. H.; Müller, P.; Becker, J. *Org. Lett.* **2017**, *19*, 2607–2609.
- (36) Structure of the parent ring system (C<sub>3</sub>H<sub>4</sub>N<sub>2</sub>): Ehrlich, H. W. *Acta Crystallogr.* **1960**, *13*, 946–952.
- (37) Methylation of related pyrazole/indazole frameworks: (a) Palmer, M. H.; Findlay, R. H.; Kennedy, S. M. F.; McIntyre, P. S. *J. Chem. Soc., Perkin Trans. 2* **1975**, 1695–1700. (b) Jaffari, G. A.; Nunn, A. J. *J. Chem. Soc., Perkin Trans. 1* **1973**, 2371–2374.
- (38) Burg, A. B. *Inorg. Chem.* **1964**, *3*, 1325–1327.
- (39) Kouakou, A.; Rakib, E. M.; Spinelli, D.; Saadi, M.; El Ammari, L. *Acta Crystallogr., Sect. E: Struct. Rep. Online* **2013**, *69*, o1603–o1604.
- (40) Le Floch, P. *Coord. Chem. Rev.* **2006**, *250*, 627–681.
- (41) Elschenbroich, C. *Organometallics*, 3rd ed.; Wiley-VCH: Weinheim, Germany, 2006.
- (42) (a) Bent, H. A. *Chem. Rev.* **1961**, *61*, 275–311. (b) Bent, H. A. *J. Chem. Educ.* **1960**, *37*, 616–624.
- (43) (a) Platz, M. S. *Acc. Chem. Res.* **1995**, *28*, 487–492. (b) Borden, W. T.; Gritsan, N. P.; Hadad, C. M.; Karney, W. L.; Kemnitz, C. R.; Platz, M. S. *Acc. Chem. Res.* **2000**, *33*, 765–771.
- (44) (a) Liu, L.; Ruiz, D. A.; Munz, D.; Bertrand, G. *Chem.* **2016**, *1*, 147–153. (b) Hansmann, M. M.; Jazzar, R.; Bertrand, G. *J. Am. Chem. Soc.* **2016**, *138*, 8356–8359. (c) Mathey, F. *Dalton Trans.* **2007**, 1861–1868.
- (45) (a) Weber, L. *Eur. J. Inorg. Chem.* **2007**, *2007*, 4095–4117. (b) Huttner, G.; Evertz, K. *Acc. Chem. Res.* **1986**, *19*, 406–413.
- (46) P–C<sub>aryl</sub> single bonds: (a) Cameron, T. S.; Dahlén, B. *J. Chem. Soc., Perkin Trans. 2* **1975**, 1737–1751. (b) Daly, J. J. *J. Chem. Soc.* **1964**, 6147–6166. P=C<sub>aryl</sub> double bonds: Appel, R.; Knoll, F. *Adv. Inorg. Chem.* **1989**, *33*, 259–361. As–C<sub>aryl</sub> single bonds: Mazhar-ul-Haque; Tayim, H. A.; Ahmed, J.; Horne, W. *J. Crystallogr. Spectrosc. Res.* **1985**, *15*, 561–571. A=C<sub>aryl</sub> double bonds: Dobbs, K. D.; Boggs, J. E.; Cowley, A. H. *Chem. Phys. Lett.* **1987**, *141*, 372–375.
- (47) Exocyclic refers to the sp<sup>2</sup>–sp<sup>2</sup> C–C bond of either the NCN pincer or NC chelate that links the imine functionality to the benzene ring. In several cases, it starts as “exocyclic” and then is incorporated into a new five-membered ring.
- (48) Examples of other stibinidenes and bismuthinidenes: (a) Vranova, I.; Alonso, M.; Lo, R.; Sedláč, R.; Jambor, R.; Ruzicka, A.; De Proft, F.; Hobza, P.; Dostál, L. *Chem. - Eur. J.* **2015**, *21*, 16917–16928. (b) Vranova, I.; Alonso, M.; Jambor, R.; Ruzicka, A.; Turek, J.; Dostál, L. *Chem. - Eur. J.* **2017**, *23*, 2340–2349.
- (49) Wiberg, K. B. *Tetrahedron* **1968**, *24*, 1083–1096.
- (50) (a) Carmody, M. P.; Cook, M. J.; Tack, R. D. *Tetrahedron* **1976**, *32*, 1767–1771. (b) Pelzer, S.; Wichmann, K.; Wesendrup, R.; Schwerdtfeger, P. *J. Phys. Chem. A* **2002**, *106*, 6387–6394.
- (51) An early paper on arsole aromaticity: Epiotis, N. D.; Cherry, W. *J. Am. Chem. Soc.* **1976**, *98*, 4365–4370.
- (52) (a) Buchwald, S. L.; Fisher, R. A.; Foxman, B. M. *Angew. Chem., Int. Ed. Engl.* **1990**, *29*, 771–772. (b) Hsu, D. P.; Warner, B. P.; Fisher, R. A.; Davis, W. M.; Buchwald, S. L. *Organometallics* **1994**, *13*, 5160–5162. (c) Ashe, A. J.; Kampf, J. W.; Al-Taweel, S. M. *J. Am. Chem. Soc.* **1992**, *114*, 372–374. (d) Ashe, A. J.; Kampf, J. W.; Al-Taweel, S. M. *Organometallics* **1992**, *11*, 1491–1496.
- (53) Chen, Z.; Wannere, C. S.; Corminboeuf, C.; Puchta, R.; Schleyer, P. v. R. *Chem. Rev.* **2005**, *105*, 3842–3888.
- (54) Simon, P.; Jambor, R.; Ruzicka, A.; Dostál, L. *Organometallics* **2013**, *32*, 239–248.
- (55) Some hypervalent analogues are known: (a) Urbanova, I.; Erben, M.; Jambor, R.; Ruzicka, A.; Jirasko, R.; Dostál, L. *J. Organomet. Chem.* **2013**, *743*, 156–162. (b) Brau, E.; Zickgraf, A.; Drager, M.; Mocellin, E.; Maeda, M.; Takahashi, M.; Takeda, M.; Mealli, C. *Polyhedron* **1998**, *17*, 2655–2668. (c) Ohkata, K.; Takemoto, S.; Ohmishi, M.; Akiba, K. *Tetrahedron Lett.* **1989**, *30*, 4841–4844.
- (56) Tokitoh, N.; Matsumoto, T.; Sasamori, T. *Heterocycles* **2008**, *76*, 981–987.
- (57) Zhao, D.; Gao, W.; Mu, Y.; Ye, L. *Chem. - Eur. J.* **2010**, *16*, 4394–4401.
- (58) Vrána, J.; Jambor, R.; Ruzicka, A.; Lycka, A.; De Proft, F.; Dostál, L. *J. Organomet. Chem.* **2013**, *723*, 10–14.
- (59) (a) Bochevarov, A. D.; Harder, E.; Hughes, T. F.; Greenwood, J. R.; Braden, D. A.; Philipp, D. M.; Rinaldo, D.; Halls, M. D.; Zhang, J.; Friesner, R. A. *Int. J. Quantum Chem.* **2013**, *113*, 2110–2142. (b) *Jaguar*, versions 7.0–9.3; Schrödinger, LLC: New York, 2007–2016.